PROCEEDINGS OF SCIENCE

From test particle simulations to cosmic-ray transport

Marco Kuhlen,[a] **Philipp Mertsch**[a] **and Vo Hong Minh Phan**[a,*]

[a] *Institute for Theoretical Particle Physics and Cosmology (TTK), RWTH Aachen University, 52056 Aachen, Germany*

E-mail: vhmphan@physik.rwth-aachen.de, marco.kuhlen@rwth-aachen.de, pmertsch@physik.rwth-aachen.de

The transport of non-thermal particles across a large-scale magnetic field in the presence of magnetised turbulence has been a long-standing issue in high-energy astrophysics. Of particular interest is the dependence of the parallel and perpendicular mean free paths $\lambda_\parallel$ and $\lambda_\perp$ on rigidity $\mathcal{R}$. We have revisited this important issue with a view to applications from the transport of Galactic cosmic rays. We have run test particle simulations of cosmic ray transport in synthetic, isotropic Kolmogorov turbulence at unprecedentedly low reduced rigidities $r_g/L_c \simeq 10^{-4}$, corresponding to $\mathcal{R} \simeq 10\,\text{TV}$ for a turbulent magnetic field of $B_{\text{rms}} = 4\,\mu\text{G}$ and correlation length $L_c = 30\,\text{pc}$. Extracting the (asymptotic) parallel and perpendicular mean free paths $\lambda_\parallel$ and $\lambda_\perp$, we have found $\lambda_\parallel \propto (r_g/L_c)^{1/3}$ as expected for a Kolmogorov turbulence spectrum. In contrast, $\lambda_\perp$ has a faster dependence on r_g/L_c for $10^{-2} \lesssim r_g/L_c \lesssim 1$, but for $r_g/L_c \ll 10^{-2}$, also $\lambda_\perp \propto (r_g/L_c)^{1/3}$. Our results have important implications for the transport of Galactic cosmic rays.

38th International Cosmic Ray Conference (ICRC2023)
26 July - 3 August, 2023
Nagoya, Japan

*Speaker

PoS(ICRC2023)146

1. Introduction

Observational evidence, e.g. data secondary-to-primary ratio of cosmic-ray intensities, strongly indicates that the transport of cosmic rays (CRs) in the Galaxy is predominantly diffusive due to interactions between these particles and magnetic turbulence [1]. Magnetic turbulence is oftentimes modelled as a spectrum of different plasma waves and interactions between waves and particles are commonly described using Quasi-Linear Theory (QLT), a perturbative approach that considers a small turbulent magnetic field $\delta\mathbf{B}$ on top of the regular background field $\mathbf{B}_0$. It can be shown that theses interactions are gyro-resonant, meaning that particles with a gyroradius r_g are scattered by plasma waves with a wavenumber $k \sim 1/r_\mathrm{g}$. This leads to the mean free paths parallel and perpendicular to $\mathbf{B}_0$, denoted as $\lambda_\parallel$ and $\lambda_\perp$, being dependent on particle rigidity [1] and the turbulence power spectrum. For ease of discussion, we introduce the reduced rigidity $r_\mathrm{g}/L_\mathrm{c}$ where $r_\mathrm{g} = pc/(eB_\mathrm{rms}) = \mathcal{R}/B_\mathrm{rms}$ is the relativistic gyroradius, L_c denotes the correlation length, p is the momentum and e the charge of the particle. For an isotropic $k^{-5/3}$ Kolmogorov power spectrum for instance, the simplest expectation is for the parallel and perpendicular mean free path to scale with rigidity in the same way while the dependence on $\delta B^2/B_0^2$ should be the opposite, $\lambda_\parallel \propto \left(r_\mathrm{g}/L_\mathrm{c}\right)^{1/3}\left(\delta B^2/B_0^2\right)^{-1}$ and $\lambda_\perp \propto \left(r_\mathrm{g}/L_\mathrm{c}\right)^{1/3}\left(\delta B^2/B_0^2\right)$ [2].

Predictions of QLT for this simple isotropic Kolmogorov turbulence, however, give $\lambda_\parallel \to \infty$ and $\lambda_\parallel \to \infty$. Various modifications of QLT have been suggested to cure this problem for $\lambda_\parallel$ [3]. The most promising suggestions are dynamical turbulence and non-linear theories, both of which lead to a broadening of the resonance condition and can hence lead to predictions of $\lambda_\parallel$ being finite. Transport in the perpendicular direction, however, is a different matter altogether. It is believed that it depends both on the transport of particles along field lines as well as the transport of the field lines itself. In fact, many theories predict a rather weak falling dependence of $\lambda_\perp/\lambda_\parallel$ not too different from the simple expectation mentioned above. Numerical simulations, however, show a different scaling of $\lambda_\parallel$ and $\lambda_\perp$. While $\lambda_\parallel$ is in agreement with the $(r_\mathrm{g}/L_\mathrm{c})^{1/3}$ behaviour generically expected for gyro-resonant interactions with Kolmogorov turbulence, the scaling of $\lambda_\perp$ with $r_\mathrm{g}/L_\mathrm{c}$ is faster. In particular, $\lambda_\perp/\lambda_\parallel \propto (r_\mathrm{g}/L_\mathrm{c})^{\Delta s}$ with $\Delta s \simeq 0.2$ and this behaviour had been indicated already in many previous works [4, 5]. We also note that at the reduced rigidities where simulation results are available, the scaling of $\lambda_\perp$ with $(\delta B^2/B_0^2)$ as indicated above is not observed either [6]. So far, neither the scaling with rigidity nor with $(\delta B^2/B_0^2)$ has been understood.

We have revisited the important question on the nature of perpendicular transport with a focus on the rigidity-dependence of $\lambda_\perp$ in isotropic turbulence. To this end, we have run a large suite of numerical test-particle simulations reaching unprecedentedly low rigidities, $r_\mathrm{g}/L_\mathrm{c} \simeq 10^{-4}$ which for $L_\mathrm{c} = 30\,\mathrm{pc}$ and $B_\mathrm{rms} = 4\,\mu\mathrm{G}$ corresponds to rigidities of $\mathcal{R} \sim 10\,\mathrm{TV}$. These small rigidities have been made possible by the use of graphics processing units (GPUs) for solving the equations of motions. We have found that the perpendicular mean free path $\lambda_\perp$ scales differently than the parallel one for $10^{-2} \lesssim r_\mathrm{g}/L_\mathrm{c} \lesssim 1$, but for $r_\mathrm{g}/L_\mathrm{c} \ll 10^{-2}$ the same rigidity-dependence is recovered.

The outline of this proceeding is as follows. In Sec. 2, we explain the preparation of an isotropic turbulent magnetic field on a computer and describe the test particle simulations. We then discuss briefly how diffusion coefficients can be derived from these simulation and afterwards present our

[1] Rigidity $\mathcal{R}$ is defined as the ratio of particle momentum p and charge q, that is $\mathcal{R} \equiv pc/q$ with the speed of light c.

results and potential phenomenological consequences. We conclude in Sec. 4.

2. Test particle simulations in isotropic turbulence

We study perpendicular transport of CRs using test particle simulations, i.e. the back-reaction of cosmic rays onto the magnetic field is neglected [6]. In these simulations, a set of test particle trajectories in a predefined magnetic field is computed by solving the Newton-Lorentz equation

$$\frac{\mathrm{d}\,\mathbf{p}}{\mathrm{d}t} = q\,\frac{\mathbf{v} \times [\mathbf{B}_0 + \delta\,\mathbf{B}(\mathbf{r})]}{c}\,, \tag{1}$$

where q is the particle charge, $\mathbf{v}$ and $\mathbf{p}$ are the velocity and momentum vectors, $\mathbf{B}_0$ is a large-scale coherent magnetic field, and $\delta\,\mathbf{B}$ represents a small-scale turbulent field. We will assume magnetostatic turbulence throughout (no time dependence on the magnetic field) and, more importantly, the electric field is neglected due to the high mobility of charges in typical astrophysical plasmas. The latter assumption also means that the particle energy is conserved and, to ensure this for the test particle trajectories in the simulations, we adopt the energy conserving Boris method in solving the Newton-Lorenz equations [7].

Concerning the turbulent magnetic field, it can be generated by magnetohydrodynamics simulations [8], but the dynamical range that can be simulated limits these simulations to normalized rigidities $r_{\mathrm{g}}/L_{\mathrm{c}} > 10^{-2}$ [9]. In order to simulate particles at sufficiently small rigidities relevant in the context of Galactic CR transport, we will rely on synthetic turbulent magnetic fields. The synthetic turbulent magnetic field considered will be a Gaussian random field that has the properties of a magnetic field and as such fulfils Maxwell's equations. In this work, we will limit ourselves to the case where the turbulent field is isotropic and follows a Kolmogorov power spectrum $g(k) \sim k^{-5/3}$ for $2\pi/L_{\max} \leq k \leq 2\pi/$ with the normalization given by $\delta B^2 = 8\pi \int_0^\infty \mathrm{d}k\, g(k)$. The overall strength of the turbulent component with respect to the total root mean square B-field can be characterized with the turbulence level $\eta \equiv \delta B^2/\left(B_0^2 + \delta B^2\right)$.

We note also that, in order to cover a large dynamical range of the power spectrum, the turbulent magnetic field is set up on a nested grid which is built by superimposing multiple grids with different sizes following the approach introduced in Ref. [10]. Essentially, plasma waves with small to large wavelengths are resolved on subgrids with small to large grid spacing. We refer interested readers to Ref. [11] for more technical details on the configuration of these subgrids. In our simulations, we are not sensitive to the individual parameter values of particle rigidity $\mathcal{R}$, the correlation length[2] L_{c} ($L_c \simeq L_{\max}/5$ for isotropic Kolmogorov turbulence) and the root mean square B-field $B_{\mathrm{rms}} = \sqrt{B_0^2 + \delta B^2}$, but only to the combination $r_{\mathrm{g}}/L_{\mathrm{c}}$. Therefore, our simulations can be applied to different combinations of these parameters. However, when considering the use for a particular physics case, e.g. transport of Galactic CRs, we often adopt fiducial parameter values. Specifically, we consider an outer scale $L_{\max} = 150\,\mathrm{pc}$ (or $L_{\mathrm{c}} \simeq 30\,\mathrm{pc}$ for Kolmogorov turbulence) [12]. With an rms value of $4\,\mu\mathrm{G}$, the gyroradius evaluates to $r_{\mathrm{g}} = 0.270\,\mathrm{pc}(\mathcal{R}/\mathrm{PV})(B_{\mathrm{rms}}/4\,\mu\mathrm{G})^{-1}$. We run these simulations on GPU in order to compute in parallel a sufficiently large number of trajectories within limited computing times and, thanks to this efficient parallelization, we can explore perpendicular transport at unprecedentedly low rigidities.

[2]The correlation length is defined such that $\int_{-\infty}^{\infty} \mathrm{d}L\, \langle \delta B(r_0) \cdot \delta B(r_0 + \Delta r(L)) \rangle \equiv L_{\mathrm{c}} \delta B^2$

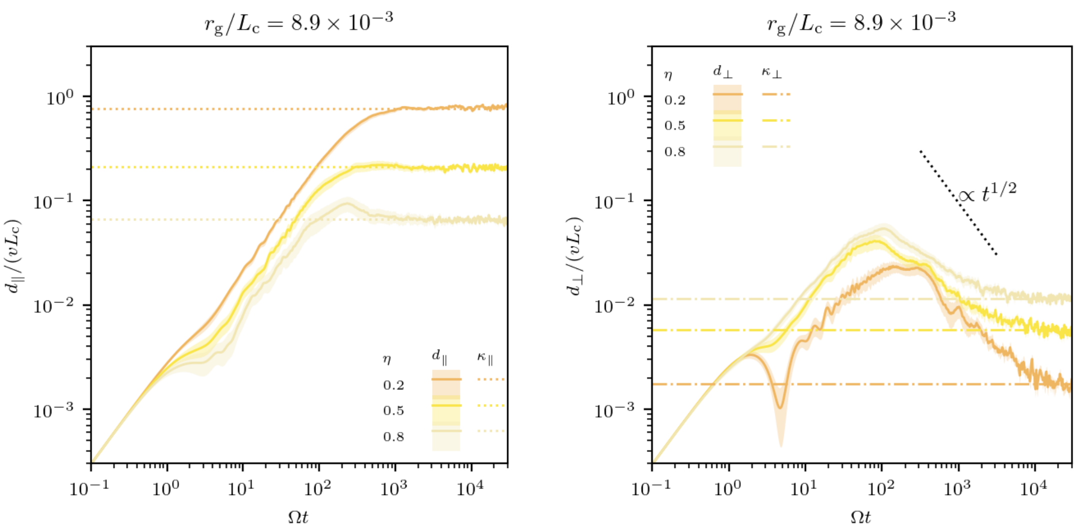

Figure 1: Left panel: Parallel running diffusion coefficient at reduced rigidity $r_g/L_c = 8.9 \times 10^{-3}$ for different turbulence level $\eta = 0.2$, 0.5, and 0.8 (see legend). Right panel: Same as in the left panel but for perpendicular running diffusion coefficient.

3. Particle diffusion coefficients

Once the test particle trajectories are computed for many different realizations of the turbulent magnetic field, they can be used to infer parameters of the transport model, such as the diffusion coefficient [4, 13], predict spectra or large-scale anisotropies [14, 15], or investigate effects beyond the standard picture of cosmic ray transport such as the generation of small-scale anisotropies in the arrival directions [16–18].

In this work, we will focus essentially on understanding the nature of particle transport in isotropic Kolmogorov turbulence which can be characterised, roughly speaking, by the time-dependence of the mean-square displacement in different directions i, $\langle(\Delta r_i)^2\rangle$. If this is of power law form, that is

$$\langle(\Delta r_i)^2\rangle = \left\langle (r_i(t) - r_i(0))^2 \right\rangle \propto t^\alpha \, , \tag{2}$$

transport is called sub-diffusive if $0 < \alpha < 1$, diffusive for $\alpha = 1$, super-diffusive for $1 < \alpha < 2$ and ballistic for $\alpha = 2$ [3, 6]. The diffusion coefficient κ, that is the constant of proportionality in Eq. (2) for the case of diffusive transport, plays a central role in the transport theory of CRs. In order to derive diffusion coefficients from test particle simulations, we have to first define the running diffusion coefficient with respect to direction i as $d_{ii}(t) \equiv \frac{1}{2}\frac{\mathrm{d}}{\mathrm{d}t}\langle (r_i(t) - r_i(0))^2\rangle$. Specifically, since the isotropy of the space is broken by the presence of a background magnetic field, here assumed to point in the z-direction, we distinguish the parallel and the perpendicular running diffusion coefficients as follows $d_\parallel(t) = d_{zz}(t)$ and $d_\perp(t) = \left(d_{xx}(t) + d_{yy}(t)\right)/2$. If transport is diffusive at late times, those converge towards the asymptotic diffusion coefficients $\kappa_\parallel \equiv \lim_{t\to\infty} d_\parallel(t)$ and $\kappa_\perp \equiv \lim_{t\to\infty} d_\perp(t)$.

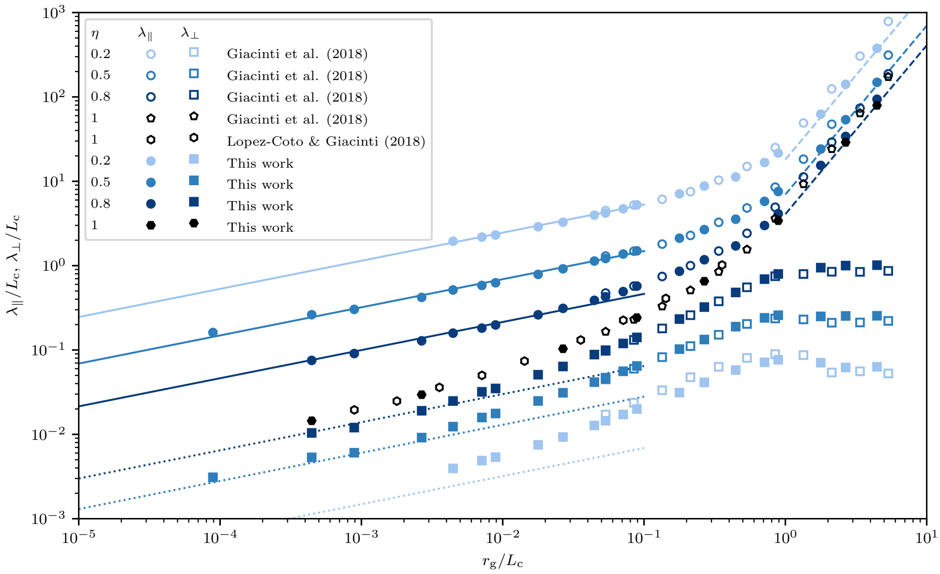

Figure 2: Asymptotic parallel and perpendicular mean free paths $\lambda_\parallel$ and $\lambda_\perp$ as a function of reduced rigidity r_g/L_c for different turbulence levels $\eta = 0.2,\ 0.5,\ 0.8$ and 1 overlaid with results from [19, 20].

3.1 Running diffusion coefficients

We start the discussions by looking at the parallel and perpendicular running diffusion coefficients which are computed from particle trajectories following the approach mentioned above. In Fig. 1, we show $d_\parallel(t)$ and $d_\perp(t)$ at reduced rigidity $r_g/L_c = 8.9\times 10^{-3}$ corresponding to rigidity of 1 PV for our fiducial parameters ($L_{max} = 150\,$pc, $B_{rms} = 4\,\mu$G) for different turbulence levels.

It is clear from the results for $d_\parallel(t)$ that there are essentially three stages of parallel transport. For $\Omega t \ll 1$, the particles are moving ballistically into their initial direction and are not yet affected by the magnetic field. The mean square displacement, e.g. in the z-direction is $\langle (z - z(0))^2\rangle = (1/3)v^2t^2$. Therefore, $d_\parallel(t) = v^2t/3$ or $d_\parallel/(vL_c) = (1/3)\Omega t\, r_g/L_c$. For $1 \ll \Omega t \ll \Omega\tau_s \simeq 3\Omega\kappa_\parallel/v^2$, particles have started to gyrate in the effective background magnetic field. While the mean-square displacement still grows $\propto t^2$, it does so with a reduced rate such that $d_\parallel(t) = Av^2t/3$ with $A < 1$. It can be shown that $A = 1 + 2\sigma_{eff}^4 - 2\sigma_{eff}^2 \coth\left(1/\sigma_{eff}^2\right)$ where $\sigma_{eff} = \arctan\left(\sqrt{\delta B^2/B_0^2}\right)$, for instance $A \simeq 0.4$ for $\eta = 0.5$ [11]. Note that we have introduced also the scattering time τ_s which marks the transition between ballistic and diffusive transport in the parallel direction. Finally, for $\Omega t \gg \Omega\tau_s$, pitch-angle scattering is reducing the mean square displacement to diffusive behaviour, $\langle (z - z(0))^2\rangle \propto t$. Consequently, the running diffusion coefficient, $d_\parallel(t)$ flattens out. The asymptotic value $\kappa_\parallel(t)$ and the transition time, of course, depend on the reduced rigidity r_g/L_c. We will discuss this rigidity-dependence in more detail in Sec. 3.2.

The time-dependence of the running perpendicular diffusion coefficient is slightly more complicated and can be described with four phases of transport which are separated by the times $\Omega t = 1$, $\Omega\tau_s$ and $\Omega\tau_c$. For $\Omega t \ll 1$, the particles are not affected by the magnetic field and move ballistically. The mean-square displacement in the x- and y-directions does not differ from the one in the z-direction and so the running diffusion coefficients are both $d_\parallel(t) = d_\perp(t) = v^2t/3$ or

$d_{\parallel}/(vL_{\rm c}) = d_{\perp}/(vL_{\rm c}) = (1/3)\Omega t\, r_{\rm g}/L_{\rm c}$. For $1 \ll \Omega t \ll \Omega\tau_{\rm s}$, particle motion does get affected by the effective background magnetic field and particles start gyrating about the effective background field direction. This is best seen at low turbulence levels, e.g. $\eta = 0.2$. There is also a suppression of the perpendicular running diffusion coefficient, but in the opposite direction: Whereas for $d_{\parallel}$, the suppression gets stronger for larger turbulence level η, for $d_{\perp}$ the suppression is larger for small η. This can be understood in the following way: In the limit $\delta B \to 0$, the motion in the x- and y-directions would be merely a gyration. A finite $\delta\mathbf{B}$ misaligns the effective magnetic field direction from the z-direction such that part of the gyration in the perpendicular plane now contributes to the parallel motion; in turn, some of the parallel ballistic motion, contributes to the transport in the x- and y-directions. The larger η, the stronger is this effect. For $\Omega\tau_{\rm s} \ll \Omega t \ll \Omega\tau_{\rm c}$, perpendicular transport is sub-diffusive, $d_{\perp} \propto t^{\alpha-1}$ with $\alpha < 1$. Here, we have introduced τ_c which marks the transition between sub-diffusive and diffusive transport. Roughly speaking, $\tau_{\rm c}$ is the time it takes for particles to transport perpendicularly by a distance of about one correlation length [21]. We note also that the subdiffusive behaviour is reminiscent of so-called compound subdiffusion [22], an effect due to diffusive particle transport along diffusive field lines. However, while compound subdiffusion predicts $d_{\perp} \propto t^{1/2}$, we do not find this scaling for all η, see the dotted line in Fig. 1. We note that the transition to this regime sets in later for smaller η as $\tau_{\rm s}$ is larger. Finally, for $\Omega\tau_{\rm c} \ll \Omega t$, perpendicular transport also becomes diffusive and $d_{\perp}$ attains its asymptotic value, $\kappa_{\perp}$.

3.2 Rigidity dependence of asymptotic diffusion coefficients

In Fig. 2 we show the mean free paths $\lambda_{\parallel} = 3\kappa_{\parallel}/v$ and $\lambda_{\perp} = 3\kappa_{\perp}/v$ as functions of rigidity, for the different turbulence levels $\eta = 0.2$, 0.5, 0.8 and 1. Note that we have derived the asymptotic values by averaging the values $d_{\parallel}$ and $d_{\perp}$ within $\Omega t_{\rm max}/2 \lesssim \Omega t \leq \Omega t_{\rm max}$ where $t_{\rm max}$ is the maximum run time for the simulations. The errors of these estimates are also obtained by averaging the standard errors of the mean within this time period. We have also plotted some lines with constant power law indices. For reduced rigidities $r_{\rm g}/L_{\rm c} \ll 1$, the asymptotic parallel diffusion coefficient $\kappa_{\parallel}$ exhibits the $(r_{\rm g}/L_{\rm c})^{1/3}$-dependence expected for gyro-resonant interactions due to turbulence with a power spectrum $g(k) \propto k^{-5/3}$. At rigidities $r_{\rm g}/L_{\rm c} \gg 1$, the $(r_{\rm g}/L_{\rm c})^2$-dependence of small-angle scattering is visible (e.g. [23]). We note that the normalisation of the diffusion coefficient decreases with increasing turbulence level η. We have also plotted the results from Ref. [19] which uses the same turbulence model. The agreement is excellent in the range where the simulation data overlap.

As far as the perpendicular diffusion coefficient is concerned, its rigidity-dependence is more complicated. Again, we show a power law $\propto (r_{\rm g}/L_{\rm c})^{1/3}$ that matches the simulation results at low rigidities. However, it appears that the data follow this dependence only over a limited rigidity range. At intermediate rigidities, $\kappa_{\perp}$ grows faster than $(r_{\rm g}/L_{\rm c})^{1/3}$; for $r_{\rm g}/L_{\rm c} \gtrsim 1$, $\kappa_{\perp}$ becomes constant. The behaviour at intermediate and large rigidities is in line with the behaviour seen in Ref. [5]. The normalisation at low rigidities shows the expected ordering in that the diffusion coefficient is smaller for smaller η. The deviation from the $(r_{\rm g}/L_{\rm c})^{1/3}$-behaviour sets in at rigidities $r_{\rm g}/L_{\rm c} \sim 10^{-2}$ for $\eta = 0.8$ and at $r_{\rm g}/L_{\rm c} \sim 3 \times 10^{-3}$ for $\eta = 0.5$. We have not actually observed the $(r_{\rm g}/L_{\rm c})^{1/3}$-scaling for $\eta = 0.2$ for the rigidities for which we were able to run simulations.

These results might have profound phenomenological consequences as some of deviations between isotropic diffusion models and spatial distribution of CRs derived from gamma-ray observations have been suggested to be due to a different rigidity-dependence of $\lambda_{\parallel}$ and $\lambda_{\perp}$ [24]. Our simulation results, however, find the same $(r_g/L_c)^{1/3}$-scaling for both $\lambda_\parallel$ and $\lambda_\perp$ at low rigidites making this hypothesis less viable in explaining these deviations.

4. Conclusion

Perpendicular transport of high-energy particles is important in a number of environments and a sound theoretical understanding is important when interpreting observations, be it of *in-situ* observations in the heliosphere, studies of Galactic CRs or non-thermal emission from sources. Our simulations have shown that the rigidity-dependence of the perpendicular mean free path $\lambda_\perp$ differs from that of the parallel mean free path $\lambda_\parallel$ for reduced rigidities $r_g/L_c \lesssim 1$; at even lower reduced rigidities $r_g/L_c \ll 1$, however, the perpendicular diffusion coefficient returns back to the same scaling. Specifically, for Kolmogorov turbulence, $\lambda_\parallel \propto (r_g/L_c)^{1/3}$ for all $r_g/L_c \lesssim 1$ and $\lambda_\perp \propto (r_g/L_c)^{0.5}$ for $10^{-2} \lesssim r_g/L_c \lesssim 1$. Previous analyses had instead speculated about the $\lambda_\perp \propto (r_g/L_c)^{0.5}$ behaviour extending to the lowest rigidities. However, our simulations at unprecedentedly low rigidities reveal that $\lambda_\perp \propto (r_g/L_c)^{1/3}$ again for $r_g/L_c \lesssim 10^{-2}$. We have provided also an analytical model in Ref. [21] that is able to reproduce this scaling as long as the subdiffusive phase in the running field line diffusion coefficient is taken into account.

References

[1] S. Gabici, C. Evoli, D. Gaggero, P. Lipari, P. Mertsch, E. Orlando et al., *The origin of Galactic cosmic rays: Challenges to the standard paradigm*, International Journal of Modern Physics D **28** (2019) 1930022 [1903.11584].

[2] D. B. Melrose, *Plasma astrophysics: Nonthermal processes in diffuse magnetized plasmas. Volume 1 - The emission, absorption and transfer of waves in plasmas*. 1980.

[3] A. Shalchi, *Perpendicular Transport of Energetic Particles in Magnetic Turbulence*, Space Sci. Rev. **216** (2020) 23.

[4] G. Giacinti, M. Kachelrieß and D. V. Semikoz, *Reconciling cosmic ray diffusion with Galactic magnetic field models*, J. Cosmology Astropart. Phys. **2018** (2018) 051 [1710.08205].

[5] A. Dundovic, O. Pezzi, P. Blasi, C. Evoli and W. H. Matthaeus, *Novel aspects of cosmic ray diffusion in synthetic magnetic turbulence*, Phys. Rev. D **102** (2020) 103016 [2007.09142].

[6] P. Mertsch, *Test particle simulations of cosmic rays*, Ap&SS **365** (2020) 135 [1910.01172].

[7] J. P. Boris, *Relativistic plasma simulation-optimization of a hybrid code*, *Proceeding of Fourth Conference on Numerical Simulations of Plasmas* (1970) .

[8] A. A. Schekochihin, *MHD Turbulence: A Biased Review*, *arXiv e-prints* (2020) arXiv:2010.00699 [2010.00699].

[9] R. Cohet and A. Marcowith, *Cosmic ray propagation in sub-Alfvénic magnetohydrodynamic turbulence*, A&A **588** (2016) A73 [1601.04971].

[10] G. Giacinti, M. Kachelrieß, D. V. Semikoz and G. Sigl, *Cosmic ray anisotropy as signature for the transition from galactic to extragalactic cosmic rays*, J. Cosmology Astropart. Phys. **2012** (2012) 031 [1112.5599].

[11] M. Kuhlen, V. H. M. Phan and P. Mertsch, *Diffusion of relativistic charged particles and field lines in isotropic turbulence*, *arXiv e-prints* (2022) arXiv:2211.05881 [2211.05881].

[12] A. Chepurnov, A. Lazarian, S. Stanimirović, C. Heiles and J. E. G. Peek, *Velocity Spectrum for H I at High Latitudes*, ApJ **714** (2010) 1398 [astro-ph/0611462].

[13] P. Reichherzer, J. Becker Tjus, E. G. Zweibel, L. Merten and M. J. Pueschel, *Turbulence-level dependence of cosmic ray parallel diffusion*, MNRAS **498** (2020) 5051 [1910.07528].

[14] G. Giacinti, M. Kachelrieß and D. V. Semikoz, *Explaining the Spectra of Cosmic Ray Groups above the Knee by Escape from the Galaxy*, *Phys. Rev. D* **90** (2014) 041302 [1403.3380].

[15] Y. Génolini and M. Ahlers, *Local Turbulence and the Dipole Anisotropy of Galactic Cosmic Rays*, *PoS* **ICRC2021** (2021) 160.

[16] G. Giacinti and G. Sigl, *Local Magnetic Turbulence and TeV-PeV Cosmic Ray Anisotropies*, Phys. Rev. Lett. **109** (2012) 071101 [1111.2536].

[17] M. Ahlers and P. Mertsch, *Origin of small-scale anisotropies in Galactic cosmic rays*, *Progress in Particle and Nuclear Physics* **94** (2017) 184 [1612.01873].

[18] M. Kuhlen, V. H. M. Phan and P. Mertsch, *No Longer Ballistic, Not Yet Diffusive-the Formation of Cosmic-Ray Small-scale Anisotropies*, ApJ **927** (2022) 110 [2111.06419].

[19] G. Giacinti and J. G. Kirk, *Large-scale Cosmic-Ray Anisotropy as a Probe of Interstellar Turbulence*, ApJ **835** (2017) 258 [1610.06134].

[20] R. López-Coto and G. Giacinti, *Constraining the properties of the magnetic turbulence in the Geminga region using HAWC γ-ray data*, *Mon. Not. Roy. Astron. Soc.* **479** (2018) 4526 [1712.04373].

[21] M. Kuhlen, V. H. M. Phan and P. Mertsch, *Field line subdiffusion and cosmic ray perpendicular transport in isotropic turbulence*, *arXiv e-prints* (2022) .

[22] G. M. Webb, G. P. Zank, E. K. Kaghashvili and J. A. le Roux, *Compound and Perpendicular Diffusion of Cosmic Rays and Random Walk of the Field Lines. I. Parallel Particle Transport Models*, ApJ **651** (2006) 211.

[23] A. Gruzinov, *Are 10 EeV cosmic rays extragalactic? Theory of cosmic ray diffusion at high energy*, 1808.00041.

[24] S. S. Cerri, D. Gaggero, A. Vittino, C. Evoli and D. Grasso, *A signature of anisotropic cosmic-ray transport in the gamma-ray sky*, J. Cosmology Astropart. Phys. **2017** (2017) 019 [1707.07694].